Frictional Resistance of a Forest Edge

B. Shannak[1], U. Corsmeier[2], Ch. Kottmeier[3], K. Träumner[4], A. Wieser[5], M. Al-Rashdan[6]

[1,2,3,4,5] Institute for Meteorology and Climate Research - Troposphere Research, Karlsruhe Institute of Technology, Hermann-von-Helmholtz-Platz 1, 76344 Eggenstein-Leopoldshafen, Germany

[1,6] Al-Balqa' Applied University (BAU), Al-Huson University College, Mechanical Engineering Department, Al-Huson P.O.BOX 50, Jordan

[1]benbellas@yahoo.com; [2]Ulrich.corsmeier@kit.edu; [3]christoph.kottmeier@kit.edu; [4]katja.traeumner@kit.edu; [5]andreas.wieser@kit.edu; [6]mmrashdan@yahoo.com

Abstract

The effect of vegetation on flow generally is expressed as an effect on hydraulic roughness. Based on wind velocity measurements using a Doppler, Wind LIDAR (Light Detection And Ranging), the resistance of forest edge and, hence, the velocity profile and friction coefficient were investigated. Against the sudden change in roughness height due to the existence of trees, the airflow streamlines are unable to follow the sharp angle of the forest. As a consequence, flow separation and contraction occur and cause the main friction losses. Considering the shape of the measured wind profiles flat, parabolic and wavy inflected profiles forms can be distinguished. Applying the conservation laws of mass, momentum, and energy, a new model was developed to determine the friction coefficient of forest. The experimental results demonstrate that at 30 m forest height and an average wind velocity from 3 up to 9 m/s the friction coefficient decreases with increasing pressure ratio and Froude number as well as Reynolds number and varies from 0.08 to 0.002. An empirical correlation was represented as a simplified form of the proposed model. The correlation includes the relevant primary parameters, fits the experimental data well, and is sufficiently accurate for engineering purposes. The results may be very useful for the most common flow dynamics problems in the atmosphere, environment, hydrology, metrology, and wind engineering.

Keywords

Friction Coefficien; Flow Resistance; Forest; Velocity Profile; LIDAR

Introduction

Forests with a high density of trees cover approximately 9.4% of the Earth's surface and are a dominant part of the environment. For people and the environment, trees provide many economic, ecological, and social benefits, such as shading and cooling. They increase property values, prevent water runoff and soil erosion, improve water quality, reduce energy use, clean the air, and enhance wildlife habitats. The effect of vegetation on flow generally is expressed as an effect on hydraulic roughness. Pressure drop is the result of frictional forces acting on the fluid as it flows through the tube. The frictional forces are caused by a resistance to flow. The main factors impacting resistance to fluid flow are fluid velocity through the pipe and fluid viscosity. Any liquid or gas will always flow in the direction of least resistance (less pressure). Friction loss has several causes, including movement of fluid molecules against each other, movement of fluid molecules against the surface, and flow separation.

It is generally agreed that vegetation increases flow resistance. Vegetation is present on a large proportion of emerged land and consequently affects the characteristics of the wind in the lower part of the atmospheric boundary layer. In the open literature, previous surveys, such as those of Raupach & Thom [1], Raupach et al. [2], Finnigan [3], and Finnigan et al. [4] focused on the effect of vegetation on wind and in particular on its turbulent features. Many reviews exist on specific aspects of the direct or indirect effects of wind on plants. Berry et al. [5] and Cleugh et al. [6] investigated the crop dynamics, whereas Gardiner [7] and Moore & Maguire [8] studied the dynamics of trees. Literature addressing flow and dispersion in urban areas is spread over many disciplines (meteorology, engineering, geography, and others), with each having a fundamental and an operational aspect, as reported by Britter & Hanna [9]. The understanding of turbulent behaviour in flowing fluids is one of the most intriguing problems in classical physics. In order to better understand the behaviour of the flow around forests, several publications focused on the investigation of turbulence and momentum losses above forests, drag forces, mechanical interactions between wind and plants, and velocity distribution of the wind above forests, such as

Oliver [10], Parlange & Brutsaert [11], De Langre [12], Lee X. [13], Frank & Ruck [14], Sellier et al. [15], Chamorro & Porté-Agel [16], Dalp & Masson [17], Dupotd & Brunet [18], Sörgel et al. [19], Dupont & Brunet [20], and Queck & Bernhofer [21]. The dynamics of air flows intrinsic to urban areas in complex terrain was reviewed by Fernando [22]. His study showed that the basic fluid dynamics played a central role in explaining observations of urban flow and in developing sub-grid parameterisations for predictive models. Vegetation flow resistance problems usually are classified into two groups:

- flow over submerged, short vegetation and
- flow through non-submerged, high vegetation

Most efforts to study vegetal resistance concentrated on studying submerged and rigid roughness. Resistance to flow through emergent vegetation can be described by simple equations that account for stem drag and, where necessary, bed shear. Therefore, Sheng & Nguyen [23] investigated the flow resistance of emergent vegetation. Values of the drag coefficient inferred from flow measurements are significantly larger than accepted values for long cylinders and show greater variation with the stem Reynolds number. In the works of Wu et al. [24] and Fu-Sheng [25], the formulas of drag coefficient and equivalent Manning's roughness coefficient were derived by analysing the force of the flow of non-submerged rigid vegetation in an open channel. The flow characteristics and mechanism of non-submerged rigid vegetation were studied by flume experiments. Unexpectedly, the roughness coefficient was found to increase with increasing Reynolds number, which does not agree with the trend in literature. Better understanding of the role of vegetation in the transport of fluid and pollutants requires improved knowledge of the detailed flow structure within the vegetation. The wind tunnel study of Burri et al. [26] examines sediment transport in live plant canopies, whereas most previous studies used model plants for this purpose. The results demonstrated that both mass flux and concentration in the air decreased exponentially with increasing canopy density, which reflects the plants' resistance.

Ogunlela & Makanjuola [27] determined the hydraulic roughness and, hence, the friction coefficient of African grasses. The control channel without any grass yielded consistently lower results than the vegetated channels. The resistance values ranged between 0.03 and 0.06. Furthermore, the results of Stephan & Gutknecht [28] indicate that the wavy motion of the plants does not increase the hydraulic resistance. A considerable number of flow resistance formulas or models have been developed so far, which treat plants simply as rigid cylinders. Branched and leafy flexible plants are far from this simplification. Several researchers used the stiffness of vegetation as a primary independent parameter to relate flow resistance to vegetation characteristics. Järvelä [29] studied the flow resistance of natural grasses, sedges, and willows in a laboratory flume, while Järvelä [30] investigated the flow resistance caused by stiff and flexible woody vegetation. The results show large variations in the friction factor with the depth of flow, velocity, Reynolds number, and vegetative density. Based on the experimental work, a better understanding of flow resistance due to different combinations of natural stiff and flexible vegetation under non-submerged and submerged conditions was gained. Friction factor values from 0.3 to 4.3 were obtained in the Reynolds number range of 24200 - 177000. Conventional resistance equations are inappropriate for flow through emergent vegetation, where resistance is caused primarily by stem drag throughout the flow depth rather than by shear stress at the bed. The work of Baptist et al. [31] describes two approaches to obtaining theoretically well-founded analytical expressions for submerged vegetation resistance. A numerical k–ε turbulence model was presented, which includes several important features of the influence of plants on flow. An alternative equation form is suggested by James et al. [32] and [33], in which the resistance coefficient is related to measurable vegetation characteristics and may incorporate bed roughness, if it is significant. For a wide range of flow depths and Reynolds numbers, the resistance coefficient varied from 0.2 to 0.8. The experimental results of Sun & Shiono [34] show that velocity distribution in the vegetation case differs considerably from that in the no-vegetation case. The boundary shear stress also is significantly reduced by the additional flow resistance caused by the vegetation at a similar relative water depth. The friction factor ranged from about 0.025 to 0.08 for Reynolds numbers from 23000 to 32000. Submerged vegetation has a significant impact on flow velocity. Current investigations also cover the impact of an increasing drag resistance and bottom roughness coefficient, but do not elucidate the characters of real submerged vegetation. To evaluate the effects of submerged vegetation at different velocities, laboratory flume

experiments were conducted by Wang & Wang [35] to characterise the effects of submerged plants on flow velocity. The relationship between the Reynolds number based on the effective height of the submerged vegetation and the resistance is a kind of trend line. The growth period has obvious effects on the values of the resistance coefficients, which are weaker in the initial growth stage and stronger in the declining growth stage. For the different vegetation's in the same vigorous growth stage, the values of these coefficients ranged from 0.001 to 1 at Reynolds numbers from 1000 to 100000. Characteristics and mechanical properties of vegetation have a considerable effect on the resistance to flow for both water in the vegetation zone of rivers and air in forest canopies. These properties were investigated by Fathi-Moghadam [36]. At flow velocities up to 1.8 m/s, the resistance coefficients for tall vegetation ranged from 0.6 to 2. An initial study to determine a friction factor model for ground vegetation was presented by Kenney [37]. The model develops a friction coefficient as a function of the Reynolds number for various percentage covers by plants. At very high Reynolds numbers from 80000 to 160000, the friction factor decreased down to very small values of about 2.10^{-7}. In the work of Abood et al. [38], a laboratory study was reported to analyse the effects of different types of vegetation, namely, Napier grass and Cattail grass, on the friction coefficient in an open channel. For Cattail grass, the value of the friction coefficient decreased with the increase of Reynolds number for all densities and all flow conditions. For Napier grass, the friction coefficient decreased with increasing values of the Reynolds number. For unsubmerged high-density vegetation, however, the value increased with the increase in Reynolds number. The reason of these contradicting results was not clearly discussed in their work. Shannak et al. [39] investigated the flow characteristics above a forest. In order to understand the behaviour of the turbulent flow around a forest, the wind velocity distribution, friction (shear) wind velocity, roughness length, stream lines, drag force and depth of the boundary layer were studied. The result demonstrated that the sharp edge of the forest should be rounded (curved cutting) to avoid energy and friction losses and damage to trees due to divergence, convergence, separation and recirculation of airflow.

In a fluid mechanics context, the most pressing problems include the treatment of atmospheric stability in forest areas and the treatment of arbitrary spatial variations in surface roughness. Forests are responsible for a substantial part of turbulent transfer of momentum, heat, and mass in the atmospheric boundary layer. Aerodynamically, Forests represent a change in roughness, porosity, and the effective height of the surface (zero plane displacement). This combination of aerodynamic changes suggests that the transition process is likely to be more complex than the changes associated with low vegetation. In total, there is sufficient information in literature about the friction losses of low vegetations. In contrast to this, there are hardly any data published for tall vegetation and plants, such as for forest trees. From a practical point of view, the flow resistance of forests should be investigated theoretically and experimentally to develop a suitable approach to determining the friction coefficient of forest. Firstly, the analytical study is presented in the next paragraph.

Theoretical Investigation

Roughness plays an important role in determining how a real object will interact with its environment. Rough surfaces usually wear more quickly and have higher friction coefficients than smooth surfaces. Over land, the individual roughness elements may be packed very closely together and then the top of these elements begins to act like a displaced surface. Generally, the trees in some canopies are located closely enough to make up a solid-looking mass of leaves, which results in a similar effect; namely, the average roof-top level begins to act on the flow like a displaced surface, as was reported by Stull [40].

In case of a sudden reduction of pipe diameter, the flow is not able to follow the sharp bend into the narrower pipe. As a result, flow separation occurs and creates re-circulating zones at the entrance of the narrower pipe. The main flow is contracted between the separated flow areas and later on, expands again to cover the full pipe area. The flow behaviour in the bottom half of the sudden contraction is relatively similar to that above a forest as presented in Fig 1. Close to the forest edge, the wind cannot abruptly change direction. Against the sudden change in the roughness height due to the existence of trees, the streamlines of the air flow are unable to follow the sharp angle of the forest. As a result, flow separation occurs and creates recirculation in the separation zones of the forest corner. The converging streamlines follow a smooth path, which results in the narrowing of the jet (flow contraction) called vena contracta. Later on, the fully developed flow expands again to

cover the forest. Hence, flow recirculation was developed in the lower part of the flow contraction and expansion region. As was expected, air flow then slows down; the flow is fully equilibrated with the upwardly substantial surface of the forest.

Solving fluid flow problems involves the application of one or more of the three basic equations of continuity, momentum, and energy. These three basic tools are developed from the law of conservation of mass, Newton's second law of motion, and the first law of thermodynamics and may be applied to investigate the friction losses of a forest. The steady flow energy equation between inlet (section 1) and outlet (section 2), Fig. 1, is given by:

$$q - w = \left(u_2 + g z_2 + \frac{P_2}{\rho_2} + \frac{V_2^2}{2} \right) - \left(u_1 + g z_1 + \frac{P_1}{\rho_2} + \frac{V_1^2}{2} \right) \quad (1)$$

where q is the specific heat transfer, w is the specific work, u is the internal energy, g is the gravitational acceleration, z is the fluid height, ρ is the fluid density, P is the static pressure, and V is the average velocity of the fluid.

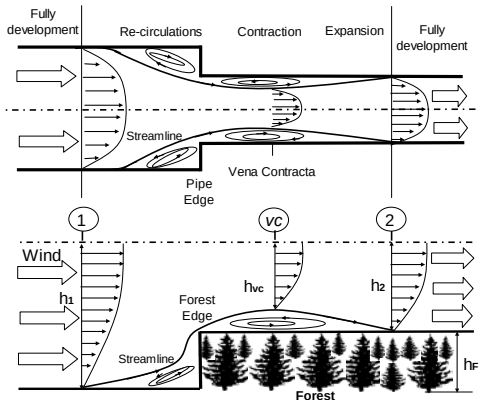

FIG. 1 SCHEMATIC OF THE TREND AND GRADIENT OF AIRFLOW STREAMLINES THROUGH SUDDEN CONTRACTION PIPE AND ABOVE FOREST EDGE

In real flow systems, losses occur due to internal and wall friction. For a forest, the frictional head loss $\Delta H_{(1\text{-}2)}$ due to the vegetated roughness surface is then defined as:

$$\Delta P_{(1-2)} = K_F \left(\frac{\rho V_2^2}{2} \right) \quad (2)$$

where K_F is the friction coefficient of the forest. The Bernoulli equation is modified to reflect these losses by adding the friction term. Applying the conservation law of mass between inlet, section (1), and outlet, section (2):

$$\rho_1 V_1 A_1 = \rho_2 V_2 A_2 \quad (3)$$

with the modified Bernoulli equation at:

- horizontal flow ($z_1 = z_2$),
- incompressible flow ($\rho_1 = \rho_2$ = constant),
- adiabatic flow ($q = 0$),
- no work done ($w = 0$), and
- one-dimensional flow

and substituting Eq. (3) and Eq. (2) in Eq. (1), the friction coefficient of the forest is therefore given as:

$$K_F = P_1 \left(\frac{2}{\rho V_1^2} \right) \left(\frac{A_2}{A_1} \right)^2 - P_2 \left(\frac{2}{\rho V_1^2} \right) \bullet \left(\frac{A_2}{A_1} \right)^2 + \left(\frac{A_2}{A_1} \right)^2 - 1 \quad (4)$$

where A_1 and A_2 are the areas of inlet and outlet, respectively. To determine the pressure at the outlet, P_2, the conservation of momentum is to be used between the inlet, section 1, and the flow contraction area, vena contracta (vc):

With the continuity equation from section (1) to section (vc)

$$V_1 A_1 = V_{vc} A_{vc}, \quad (5)$$

and the continuity equation from section (vc) to section (2)

$$V_{vc} A_{vc} = V_2 A_2 \quad (6)$$

and the definition of the contraction coefficient Cc as:

$$Cc = \frac{A_{vc}}{A_2} \quad (7)$$

and applying the momentum equation between section (1) and (vc), the outlet pressure is then

$$P_2 = P_{vc}\ Cc - \rho V_1^2 \left(\frac{A_1}{A_2} \right)^2 + \rho V_1^2 \left(\frac{A_1}{A_2} \right)^2 \left(\frac{1}{Cc} \right) \quad (8)$$

The unknown P_{vc} is the pressure at the vena contracta and should be determined by applying the Bernoulli equation for a friction-less flow from section (1) to the section of the vena contracta (*vc*) as:

$$P_{vc} = P_1 + \frac{\rho V_1^2}{2}\left(\frac{A_1}{A_2}\right)^2 - \frac{\rho V_1^2}{2}\left(\frac{A_1}{A_2}\right)^2\left(\frac{1}{Cc}\right)^2 \quad (9)$$

Substituting of Eq. (8) and Eq. (9) by Eq. (4) leads to

$$K_F = P_1\left(\frac{2}{\rho V_1^2}\right)\left(\frac{A_2}{A_1}\right)^2(1-Cc) + \left(\frac{A_2}{A_1}\right)^2(1-Cc) - \left(\frac{1}{Cc}\right) + 1 \quad (10)$$

Eq. (10) includes the influencing parameters of atmospheric pressure, wind velocity, flow density, area ratio, and contraction coefficient. Consequently, velocity measurements are necessary. In total, the forest friction coefficient K_F can be determined well based on LIDAR measured velocity profiles. The required experimental set-up is described in the next paragraph.

Experimental Investigation

Experimental Set-up

A WindTracer Doppler LIDAR manufactured by Lockheed Martine Coherent Technologies was used to measure the wind field across a forest edge. The major exterior system includes the scanner head, the air conditioner, GPS antenna, and the boxes of filter, data, and mains power. The air conditioner unit provides for an environmental control of the shelter. It is designed to minimise the amount of air exchanged from the outside to the inside of the shelter and to reduce the build-up of humidity on the system. The equipment shelter contains the Doppler LIDAR equipment and is the location of remote sensing. The environmental equipment shelter includes the scanner, the transceiver, and the signal processor. The laser radiation emanates from the transceiver and is directed into the atmosphere by the computer-controlled scanner. The backscattered laser radiation is collected and processed by the transceiver, control electronics, and signal processor to produce various data products. These data products are then displayed locally and/or broadcast to other locations. The environmental equipment shelter is connected to the remaining equipment locations via an Ethernet connection. The Remote Operator Station contains the primary Doppler LIDAR remote control and monitoring station and is connected to the shelter via an Ethernet connection. RASP-GUI stands for Real-time Advanced Signal Processor (RASP) Graphical User Interface (GUI). According to the systems operation manual [41], the WindTracer has a peak power of 4.5 kW with a pulse repetition frequency of 500 Hz. The nominal parameters of interest at the exit aperture of the scanner are listed in Table 1.

TAB. 1 NOMINAL WINDTRACER SPECIFICATIONS
PARAMETER VALUE

Laser Wavelength	**2.0**	**μm**
Laser Pulse Energy	2.0	mJ
Pulse Width	425	ns
Pulse Repetition Frequency	500	Hz
Average Power	1.0	W

The basic operation of the WindTracer is presented in Fig. 2. A pulsed laser light is generated and emitted into the atmosphere. As the light travels away from the system, small portions of the light are reflected back to the system by very small particles in the air, called aerosols. This pulse of light leaves the laser and when the reflected light is returned, distance to the particle that reflected the light can be determined. In addition, by measuring the frequency of the original pulse and the frequency of the reflected light, a shift in frequency can be measured (called a Doppler shift). The Doppler shift is induced by the component of the wind velocity of the particle directly towards or away from the laser. By analysing the frequency shift, the radial component of wind velocity of the aerosol particle is measured directly. The length of the pulses transmitted by the system is in the 50-100 m range and pulses are transmitted roughly 500 times per second. This means that the beam is a series of pencils that are emitted every 2 milliseconds and 50-80 m long and 10-30 cm wide depending on the distance from the system. LIDAR accuracy generally is stated in vertical direction, as the horizontal accuracy is controlled indirectly by the vertical accuracy. This is also due to

the fact that determination of horizontal accuracy for LIDAR data is difficult due to the difficulty of locating ground control points (GCPs) corresponding to the LIDAR coordinates. Vertical accuracy is determined by comparing the (z) coordinates of data with the truth elevations of a reference (which generally is a flat surface). The LIDAR accuracy is given as RMSE (root mean square error) and about 0.196 m. Generally, the LIDAR records a wind velocity range from 0 to 60 m/s with an accuracy of about 0.2 m/s. To estimate a random error, the autocorrelation function of the measured velocity was calculated. Under optimal LIDAR conditions, that is, a clear, but aerosol-loaded non-turbulent atmosphere, the WindTracer has an uncorrelated error of less than 0.15 m/s. Hence, the uncertainty of the measured wind velocity and the shear wind velocity was ± 0.1 and ± 0.15 per cent, respectively.

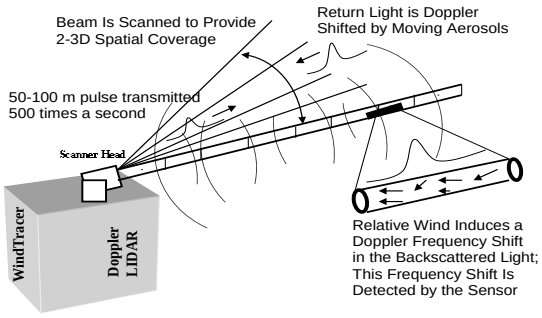

FIG. 2 BASIC PRINCIPLE OPERATION OF THE WINDTRACER

Results and Discussion

To measure the wind field across a forest edge using Doppler LIDAR, a field campaign was performed at Hatzenbühl (southwest Germany) in the winter of 2010/2011. This place was chosen due to its ideal location, measurements conditions, free grass field, and suitable forest height. The chosen forest edge has a length of about 1.8 km and is aligned nearly perpendicular to the main wind flow direction. The measurement site was located approximately 1.5 km away from the edge in a harvested field. The wind velocity is measured in 120 so-called range gates along the laser beam with a length of 60 m each, which can be freely arranged from about 350 m to 10 km away from the LIDAR instrument. The line-of-sight wind velocity is measured with a precision of about 15 cm per s in the high signal-to-noise-range. The wind speed varied from 3 to 9 m/s. The LIDAR was located 1230 m away from the forest edge, Fig 3.

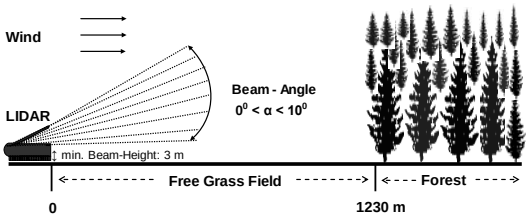

FIG. 3 SCHEMATIC OF THE LIDAR AND THE INVESTIGATED FOREST

A series of experiments using the LIDAR instrument was conducted to measure the wind speed profile above the free grass field and the forest. As an example, Fig. 4 shows a measured velocity profile of the wind in front of the forest as a function of the altitude (height) and the distance (fetch). The velocity profiles in wind direction are measured along the fetch in a LIDAR beam angle range from 0^o to 10^o. In fluid dynamics, the no-slip condition for viscous fluids states that at a solid boundary, the fluid will have zero velocity relative to the boundary. Hence, as shown in Fig. 4, the wind speed above the grass field varies approximately logarithmically with height in the surface layer at a distance of about 400 m from the LIDAR up to 1230 m.

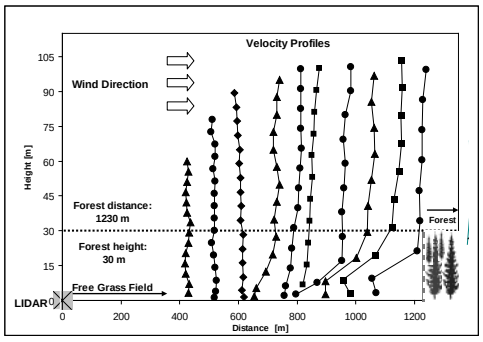

FIG. 4 MEASURED VELOCITY PROFILE OF THE WIND ABOVE GRASS FIELD AS A FUNCTION OF THE HEIGHT AND THE DISTANCE

Frictional drag causes the wind speed to decrease to zero close to the ground, while the pressure gradient force causes the wind to increase with height. The logarithmic velocity distribution appears to be universal in character, determined only by the ground condition and the distance from the ground. Flow separation occurs when the boundary layer travels far enough against an adverse pressure gradient, such that the speed of the boundary layer falls almost to zero. The air flow is detached from the ground surface near the forest, called detached region, and instead assumes the forms of eddies and vortices in the eddies region from 1000 to 1230 m. This is clearly visible by the significant decrease of the velocity and the change

of the profile shape at the lower corner before the forest.

Fig. 5 shows a measured velocity profile of the wind above the forest as a function of the height and the distance. The velocity profiles in wind direction are also measured along the fetch at a LIDAR beam angle ranging from 0^o to 10^o. The wind speed above the forest varies approximately logarithmically with height in the surface layer. At a distance of more than 1230 m, frictional drag causes the wind speed to drop to zero close to the surface of the forest, while the pressure gradient force causes the wind to increase with height. As a result, the main flow is contracted and later on, it expands again to cover the forest. Hence, flow recirculation developed in the lower part of the flow contraction and expansion region. As expected, the air flow then slows down.

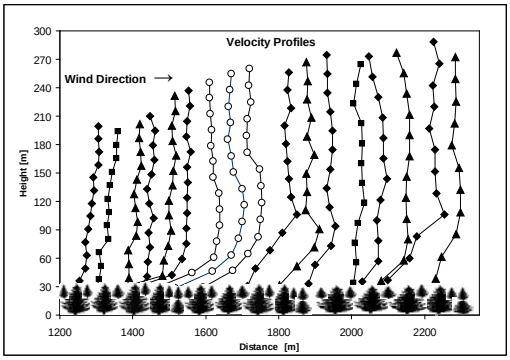

FIG. 5 MEASURED VELOCITY PROFILE OF THE WIND ABOVE FOREST AS A FUNCTION OF THE HEIGHT AND THE DISTANCE

Generally, there is random mixing between the layers of fluid in the turbulent flow. Due to this mixing, the velocity distribution is much more uniform. As a consequence, mixing has a positive effect on heat transfer. The negative effects of mixing are velocity and pressure fluctuations that may induce a heterogeneous flow distribution and, hence, different flow types. Considering the shape of the measured wind profiles above the forest in Fig. 5, three different shapes can be distinguished:

1. Flat profiles
2. Parabolic profiles
3. Wavy inflected profiles

The general shape of first profile type is similar to that of a profile over a smooth plate. The velocity profile does not seem to be parabolic, but is flatter and located 1230 to 1500 m above the forest. The parabolic profiles exist from 1500 to 1700 m and indicate the flow contraction (vena contracta). These profiles are marked by circle symbols in Fig. 5. The wavy inflected profiles are located at a distance of more than 1700 m and reflect flow expansion. However, the velocity profiles exhibit a peak in front. As expected, air flow then slows down downstream of the expansion area and the wavy inflected profile is quickly replaced by a flat profile type, the known logarithmic one. The profile is fully equilibrated with the upwardly substantial surface of the forest. The reason for the different types is that the fluid streamlines cannot abruptly change direction. In the case of both air flow above the ground of the open grassland and against the sudden change in roughness height due to the existence of trees, the streamlines are unable to follow the sharp angle of the forest. The converging streamlines follow a smooth path, which results in the narrowing of the jet (flow contraction). The ratio of the fetch above the forest and the height of the forest is defined as a forest ratio (x/h_f). The contraction region was identified in a fetch of 200 m above the forest, which corresponds to a forest ratio of about 7. In aerodynamics, flow separation may often result in increased drag, particularly pressure drag, which is caused by the pressure difference between the front of the forest and the rear surfaces of the ground as it travels through the fluid.

Figs. 6a, 6b, and 6c present three selected wind velocity profiles in front of the forest, at the vena contracta, and expansion area, respectively. Comparison of the wind profiles at distances of 1000 m (Fig. 6a), 1700 m (Fig. 6b), and 2100 m (Fig. 6c) from the LIDAR clearly shows the influence of the forest on the wind velocity distribution, the shape of the wind velocity profile, and, hence, on the flow characteristics. Collectively, the values of the wind velocity measured as a function of the altitude and fetch were in the range of > 0 to < 8 m/s. The average wind velocity obtained from the measured data ranged between 5 and 6 m/s, with the maximum wind velocity being in higher range from about 6 to 8 m/s.

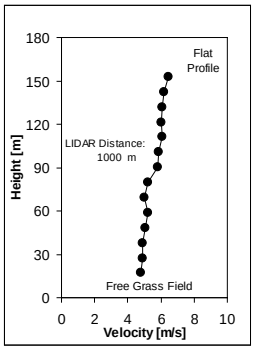

FIG. 6a FLAT PROFILE TYPE ABOVE THE FREE GRASS FIELD

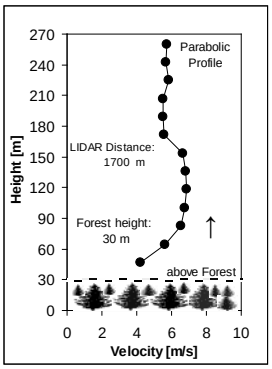

FIG. 6b PARABOLIC PROFILE TYPE ABOVE THE FOREST

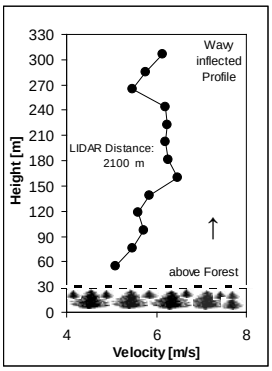

FIG. 6c WAVY INFLECTED PROFILE TYPE ABOVE THE FOREST

Model Evaluation

The forest friction coefficient K_F applied in Eq. (10) is determined based on the measured data and the following definitions:

The velocity represents the average wind velocity and the pressure is the atmospheric pressure. According to Fig.1 and Eq. (10), the wind flow above the free grass field and the forest is simplified as wind flow through a sudden contraction rectangular channel. Hence, the forest characterises the obstruction in the channel. The ground surface of the free grass field and that of the forest indicate the lower bound (wall) of Section (1) and (2), respectively. The upper bound is the top of the planetary boundary layer in the atmosphere between 1 km and the earth's surface where friction affects wind speed and wind direction. Due to the same width of the rectangular sections (b_1=b_2), the area ratio in Eq. (10) then is defined as:

$$\left(\frac{A_2}{A_1}\right)=\left(\frac{b_2\,h_2}{b_1\,h_1}\right)=\left(\frac{h_2}{h_1}\right) \qquad (11)$$

where h_1 is the height between the free ground surface and the planetary boundary layer of 1km and h_2 is height between the forest surface and the planetary boundary, defined as

$$h_2 = h_1 - h_F \qquad (12)$$

where h_F is the height of the forest. The contraction coefficient defined by Eq. (7) was determined using Eqs. (6) and (12) as well as the averaged values of the measured velocities in sections 1, *vc*, and 2. In Eq. (10), the terms (P_1) and ($\rho V^2/2$) represent the static and dynamic pressure, respectively. Fig. 7 shows the forest friction coefficient K_F as a function of the pressure ratio (static pressure/dynamic pressure).

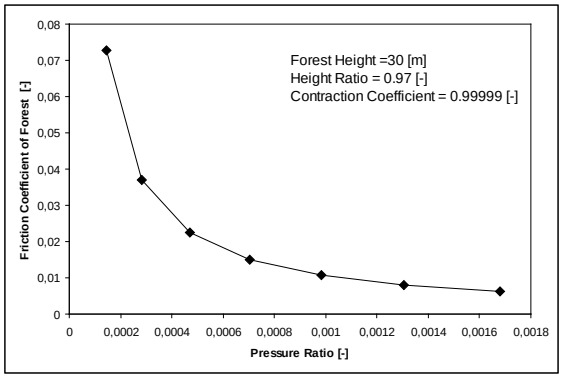

FIG. 7 FOREST FRICTION COEFFICIENT K_F AS A FUNCTION OF THE PRESSURE RATIO (STATIC PRESSURE/DYNAMIC PRESSURE)

At a forest height of 30 m, height ratio of 0.97, and contraction coefficient of 0.99999, the friction coefficient of the forest decreases from 0.07 to 0.005 with an increasing pressure ratio from 0.0002 to 0.0017. At higher wind velocity and pressure difference, the relation between the friction coefficient and the pressure ratio is less significant due to minor forest resistance. At a higher pressure ratio, the friction factor therefore remains constant at a value of about 0.002.

Based on the above experimental results and Eq. (11) as well as Eq. (12), determination of the friction coefficient by Eq. (10) is simplified to:

$$K_F = \left(\frac{2}{Fr^{\,2}}\right)\left(\frac{h_1 - h_F}{h_1}\right)^2 10^{-5} \qquad (13)$$

with the planetary boundary layer h_1 of about 1000 m, contraction coefficient of 0.99999, and F_r is the Froude number defined as:

$$Fr^{\,2} = \left(\frac{V_1^{\,2}\,\rho}{P_1}\right) \qquad (14)$$

However, Eq. (13) includes the relevant primary parameter. These are the atmospheric pressure, wind velocity, density of the air, and height of the forest:

$$K_F = f(P_1, V_1, \rho, h_F) \qquad (15)$$

The reproductive accuracy of the proposed correlation, Eq. (13), is to be tested using the data presented in this work and the literature data.The friction coefficient of the forest determined by Eq. (13) is presented in Fig.8 as a function of the Froude number and forest height. It can be seen that the friction coefficient decreases with increasing Froude number and forest height. At a forest height of 30 m, the empirical correlation, Eq. (13), fits the experimental data very well. The standard deviation of the data is about 0.03 %.

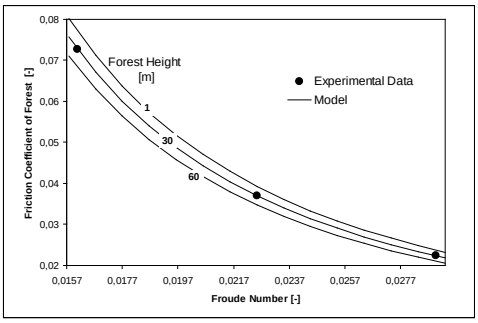

FIG. 8 FRICTION COEFFICIENT OF FOREST DETERMINED BY EQ. (13) AGAINST FROUDE NUMBER AND FOREST HEIGHT

The result obtained from the experimental data and the proposed correlation is compared with data in literature given as a function of the Reynolds number. Own data are plotted against the Reynolds number defined as:

$$Re = \frac{\rho V h_F}{\mu} \qquad (16)$$

where μ is the dynamic viscosity of the air and the height of the forest h_F of 30 m is taken to be a characteristic length. The presented data are compared with literature data for vegetation in Fig. 9.

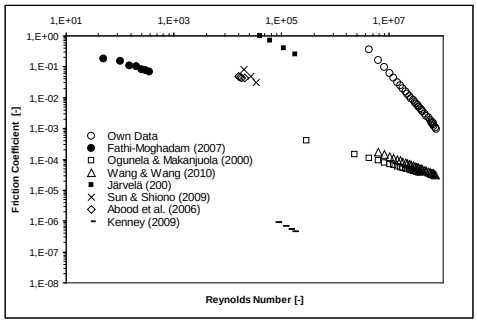

FIG. 9 FRICTION COEFFICIENT AS A FUNCTION OF REYNOLDS NUMBER

Generally, the friction coefficient is inversely proportional to the Reynolds number. All data exhibit the trend expected. The height of the vegetation investigated in literature of less than 10 m is lower than that of the investigated forest of about 30 m. Hence, the friction coefficient of the own data is larger than that given in literature. When extrapolating all data at low and high Reynolds numbers, the own data are located above the literature data of Wang & Wang [35], Ogunela & Makanjuola [27], Fathi-Moghadam [36], Kenney [37], Abood et al. [38], Järvelä [29], and Sun & Shiono [34]. The data in literature were obtained at different parameters:

- Geometrical parameters of the investigated vegetation. These are length, height, width, edge structures, and shapes of the plants as well as actual porosity, active area, and volume and especially the surface roughness of the vegetation.
- Flow parameters: velocity, quality, density, and temperature of the air and atmospheric pressure, pressure distribution, wind direction, and flow type.
- Measurement parameter: time, conditions, method, and devices of measurements.

Despite different investigation methods and geometrical and flow parameters, the data presented at very high Reynolds numbers are relatively close to the data given in the open literature.

Trees can sustain damage from many different sources. Heavy snows, strong winds, and flooding may cause major injuries at different points in tree development. To prevent such trees damage due to the strong wind, the sharp edge of the front area of the forest should be rounded or the front trees may be shortened. This may decrease the slope of the boundary layer and the streamlines in front of, above, and behind the forest. Consequently, the convergence (contraction), divergence (expansion), separation, and recirculation of the air flow can also be decreased and, hence, a less energy loss, friction loss, turbulence interchange, mass transfer, and heat transfer may occur.

Conclusion

This study focused on the theoretical and experimental investigation of the flow resistance above a forest. The velocity profiles measured by a LIDAR were analysed to determine the friction coefficient of forest. A series of experiments was conducted to measure the wind

speed profile above a forest. The frictional drag caused the wind speed to drop to zero close to the surface of the forest, while the pressure gradient force caused the wind to increase with height. The main flow is contracted and later on, expands again to cover the forest. Hence, flow recirculation developed in front of the forest and in the lower part of the flow contraction area (vena contracta). In terms of the shape of the measured wind profiles, flat, parabolic, and wavy inflected profiles were distinguished. The wind flow above the free grass field and the forest was simplified as a wind flow through a suddenly contracted rectangular channel. A theoretical model simplified to an empirical relation was developed to calculate the friction coefficient of the forest. The average velocity from 3 to 9 m/s induced a friction coefficient from 0.08 to 0.002. The correlation includes the relevant primary parameters of atmospheric pressure, density of the air flow, wind velocity, and height of the forest. Therefore, it fits the experimental data very well. The standard deviation of the data is less than 0.03 %. Despite different investigation methods and geometrical and flow parameters, the data presented are relatively close to the data published in literature. It was generally agreed that vegetation increases flow resistance. It may be of interest to modify the edge region in order to reduce wind-induced risks. The sharp edge of the forest front could be rounded or the front trees may be shortened to prevent energy and friction losses and tree damage due to the convergence, divergence, separation, and recirculation of the air flow. Better understanding of the role of vegetation in the transport of fluid and pollutants requires improved knowledge of the detailed flow structure and resistance within the vegetation.

Notation

A	area (m2)
b	width (m)
Cc	contraction coefficient (-)
d	diameter (m)
Fr	Froude number
g	gravitational acceleration (m/s2)
h	height (m)
K_F	friction coefficient of forest (-)
P	pressure (N/m2)
q	specific heat transfer (J/kg)
u	internal energy (J/kg)
Re	Reynolds number (-)
V	velocity (m/s)
w	specific work (J/kg)
x	fetch (m)
z	height above the ground (m)

Greek Symbols

ρ	density (kg m^{-3})
μ	dynamic viscosity (kg/ms)

Subscripts

1	inlet section
2	outlet section
c	contraction
F	forest
vc	vena contracta

ACKNOWLEDGMENT

This work was carried out during eht sabbatical leave granted to Prof. Shannak Benbella from Al-Balqa' Applied University (BAU), Al-Huson University College, Mechanical Engineering Department, in the academic year 2011/2012. The work was completed at the Institute of Meteorology and Climate Research, Karlsruhe Institute for Technology (KIT), Germany. The corresponding author is grateful to Prof. Ch. Kottmeier who provided outstanding technical and logistical support during the sabbatical leave. All members of the troposphere research team are acknowledged for valuable comments and discussion as well as for the measured data used in this paper.

REFERENCES

Abood, M. M., Yusuf, B., Mohammed, T. A. and Ghazali, A. H., "Manning roughness coefficient for grass-lined channel," Suranaree J. Sci. Technology, vol. 13, No. 4, pp. 317-330, 2006.

Baptist, M. J., Babovic, V., Uthurburu, J., Rodríguez, J. and Keijzer M., Uittenbogaard, R.E., Mynett, A. and Verwey, "On inducing equations for vegetation resistance," Journal of Hydraulic Research, vol. 45, No. 4, pp. 435-450, 2007.

Berry, P., Sterling, Spink, M., J., Baker, C. and Sylvester-Bradley, R.," Understanding and reducing lodging in cereals," Advances in Agronomy, vol. 84, pp. 217–71, 2004.

Britter, R. E., Hann, S. R. Flow and Dispersion in Urban Areas. Annual Review Fluid Mechanics, 2003, 35, 469–496.

Burri, K., Gromke, C., Lehning, M. and Graf, M., "Aeolian sediment transport over vegetation canopies: A wind tunnel study with live plants," Aeolian Research, doi:10.1016/j.aeolia.2011.01.003. 2011.

Chamorro, L. P. and Porté-Agel, F., Wind velocity and surface shear stress distributions behind a rough-to-smooth surface transition, A Simple New Model," Boundary-Layer Meteorol, vol. 130, pp. 29–41, 2008.

Cheng N. and Nguyen H. T., "Hydraulic radius for evaluating resistance induced by simulated emergent vegetation in open channel flows," Journal of Hydraulic Engineering, doi:10.1061/ (ASCE) HY.19437900.0000377, 2010.

Cleugh, H., Miller, J. and Böhm, M.," Direct mechanical effects of wind on crops," Agroforestry Systems, vol. 41, pp. 85–112, 1998.

Dalpě, B. and Masson, C., "Numerical simulation of wind flow near a forest edge," Journal of Wind Engineering and Industrial Aerodynamics, vol.97, pp. 228-241, 2009.

Dupont, S. and Brunet, Y., " Coherent structures in canopy edge flow: a large-eddy simulation study," J. Fluid Mechanics, vol. 630, pp. 93–128, 2009.

Dupont, S. and Brunet, Y., "Impact of forest edge shape on tree stability: a large-eddy simulation study," Forestry, vol. 81, No. 3, pp. 299-315, 2010.

Fathi-Moghadam, M., "Characteristics and mechanics of tall vegetation for resistance to flow," African Journal of Biotechnology, vol. 6, No. 4, pp. 475-480, 2007.

Fernando, H. J. S., "Fluid Dynamics of Urban Atmospheres in Complex Terrain," Annu. Rev. Fluid Mechanics, vol. 42, pp. 365–389, 2010.

Finnigan, J., Shaw, R. and Patton, E.G., "Turbulence structure above a vegetation canopy," J. Fluid Mechanics, vol. 637, pp. 387–424, 2009.

Finnigan, J., "Turbulence in plant canopies," Annual Review Fluid Mechanics, vol. 32, pp. 519–571, 2000.

Frank, C. and Ruck, B., " Numerical study of the airflow over forest clearings," Forestry," vol. 81, No. 3, pp. 259-277, 2008.

Fu-Sheng W. U., "Characteristics of flow resistance in open channels with non-submerged rigid vegetation," Journal of Hydrodynamics, vol. 20, No. 2, pp. 239-245, 2008.

Gardiner, B. A., "The interactions of wind and tree movement in forest canopies," Wind and Trees, chap. 2, pp.41–59 Cambridge Univ. Press, 1995.

James, C. S., Birkhead, A. L., Jordanova, A. A. and O'Sullivan, J. J., "Flow resistance of emergent vegetation," Journal of Hydraulic Research, vol. 42, No.4, pp. 390-398, 2004.

James, C. S., Goldbeck, U., Patini, A. and Jordanova, A. A., "Influence of foliage on flow resistance of emergent vegetation," Journal of Hydraulic Research, vol. 46, No. 4, pp. 536-542, 2008.

Järvelä, J., "Determination of flow resistance caused by non-submerged woody vegetation," International Journal of River Basin Management, vol. 2, No. 1, pp. 61-70, 2004.

Järvelä, J., "Flow resistance of flexible and stiff vegetation: a flume study with natural plants," Journal of Hydrology, vol. 269, pp. 44–54, 2002.

Kenney, P. M., "An initial study to determine a friction factor model for ground vegetation," Ph.D. Dissertation, University of Toledo, 2009.

Langre, E. De, " Effects of Wind on Plants," Annual Review of Fluid Mechanics, vol. 40, pp. 41-168, 2008.

Lee X. X., "Air motion within and above forest vegetation in non-ideal conditions," Forest Ecol. Manag., vol. 135, pp.3–18. 2000.

Moore, J. and Maguire, D., "Natural sway frequencies and damping ratios of trees: concepts, review and synthesis of previous studies," Trees Struct. Funct., vol. 18, pp. 195–203, 2004.

Ogunlela, O. and Makanjuola, M. B., Hydraulic Roughness of some African Grasses," J. agric. Engng Research, vol. 75, pp. 221-224, 2000.

Oliver, H. R., "Wind profiles in and above a forest canopy," Quarterly Journal of the Royal Meteorological Society, vol. 97, pp. 548-553, 1971.

Parlange, M. and Brutsaert, W., "The regional roughness of the landes forest and surface shear stress under neutral

conditions" Boundary – Layer Metrology, vol. 48, pp. 69-81, 1988.

Queck, R. and Bernhofer, C., "Constructing wind profiles in forests from limited measurements of wind and vegetation structure" Agricultural and Forest Meteorology, vol. 150, pp. 724–735, 2010.

Raupach, M. R., Finnigan, J. J and Brunet, Y., "Coherent eddies and turbulence in vegetation canopies, the mixing-layer analogy," Bound. Layer Meteorology, vol. 78, pp. 351–382, 1996.

Repack, M. and Thom, A., "Turbulence in and above plant canopies," Annual Review Fluid Mechanics, vol.13, pp. 97–129, 1981.

Sellier, D., Brunet, Y. and Fourcaud, T. A., "A numerical model of tree aerodynamic response to a turbulent airflow," Forestry, vol. 8, No. 3, pp. 270-297, 2008.

Shannak, B., Corsmeier, U., Kottmeier, Ch., Träumner, K. and Wieser, A.," Flow characteristics above a forest using light detection and ranging measurement data," Proc.IMechEVol 226 Part C: J. Mechanical Engineering Science, vol. 4, pp. 921-939, 2012.

Sörgel, M. S., Trebs, I., Serafimovich, A., Moravek, A., Held, A. and Zetzsch, C., "Simultaneous HONO measurements in and above a forest canopy: influence of turbulent exchange on mixing ratio differences," Atmos. Chem. Phys, Discuss 10, pp. 21109–21145, 2010.

Stephan, U. and Gutknecht, D., "Hydraulic resistance of submerged flexible vegetation," Journal of Hydrology, vol. 269, pp. 27–43, 2002.

Stull, R. B., "An Introduction to Boundary Layer Meteorology,"Kluwer Academic Publishers, Boston, Netherlands, 1988.

Sun X. and Shiono, K., "Flow resistance of one-line emergent vegetation along the floodplain edge of a compound open channel," Advances in Water Resources, vol. 32, pp. 430-438, 2009.

Tracer, Wind. System Operation User Manual. CLR Photonics, Inc, Document Nr 2FM0002851 REV A: 1-155, 2003.

Wang P. F. and Wang C. H., "Hydraulic resistance of submerged vegetation related to effective height," J. of Hydrodynamics, vol. 22, N. 2, pp. 265-273, 2010.

Wu F. C., Shen H. W. and Chou Y. J., "Variation of roughness coefficients for unsubmerged and submerged vegetation," Journal of Hydraulic Engineering, vol. 125, No. 9, pp. 934–942, 1999.